Published OnlineFirst December 20, 2011; DOI:10.1158/1940-6207.CAPR-11-0121

Cancer Prevention Research

Silencing *hsp25/hsp27* Gene Expression Augments Proteasome Activity and Increases CD8 $^{+}$ T-Cell–Mediated Tumor Killing and Memory Responses

Ganachari M. Nagaraja, Punit Kaur, William Neumann, et al.

Cancer Prev Res 2012;5:122-137. Published OnlineFirst December 20, 2011.

Published OnlineFirst December 20, 2011; DOI:10.1158/1940-6207.CAPR-11-0121

Research Article

Cancer Prevention Research

Silencing *hsp25/hsp27* Gene Expression Augments Proteasome Activity and Increases CD8$^+$ T-Cell–Mediated Tumor Killing and Memory Responses

Ganachari M. Nagaraja[1], Punit Kaur[1], William Neumann[1], Edwina E. Asea[1], María A. Bausero[2], Gabriele Multhoff[3], and Alexzander Asea[1]

Abstract

Relatively high expression of Hsp27 in breast and prostate cancer is a predictor of poor clinical outcome. This study elucidates a hitherto unknown mechanism by which Hsp27 regulates proteasome function and modulates tumor-specific T-cell responses. Here, we showed that short-term silencing of Hsp25 or Hsp27 using siRNA or permanent silencing of Hsp25 using lentivirus RNA interference technology enhanced PA28α mRNA expression, PA28α protein expression, and proteasome activity; abrogated metastatic potential; induced the regression of established breast tumors by tumor-specific CD8$^+$ T cells; and stimulated long-lasting memory responses. The adoptive transfer of reactive CD8$^+$ T cells from mice bearing Hsp25-silenced tumors efficiently induced the regression of established tumors in nontreated mice which normally succumb to tumor burden. The overexpression of Hsp25 and Hsp27 resulted in the repression of normal proteasome function, induced poor antigen presentation, and resulted in increased tumor burden. Taken together, this study establishes a paradigm shift in our understanding of the role of Hsp27 in the regulation of proteasome function and tumor-specific T-cell responses and paves the way for the development of molecular targets to enhance proteasome function and concomitantly inhibit Hsp27 expression in tumors for therapeutic gain. *Cancer Prev Res; 5(1); 122–37. ©2011 AACR.*

Introduction

The 25-kDa Hsp25 belongs to the family of small HSPs and is the murine homologue of human Hsp27, which was originally identified as an estrogen-responsive gene in breast cancer cells (1). Unlike the large HSPs, which function through ATP-dependent mechanisms, Hsp25/27 operates through ATP-independent mechanisms (2, 3). Importantly, elevated Hsp27 levels have been found in various tumors, including breast, prostate, gastric, uterine, ovarian, head and neck, and tumors, arising from the nervous system and urinary system (4). In estrogen receptor (ER)-α–positive benign neoplasia, elevated levels of Hsp27 have been shown to promote the progression to more malignant phenotypes (5). These studies were supported by findings that show that enhanced Hsp27 protein in breast cancer cells correlated well with increased anchorage-independent tumor growth (6), increased resistance to chemotherapeutic drugs (including cisplatin and doxorubicin), and increased metastatic potential *in vitro* (7–9). Together, these studies predict that elevated Hsp27 in breast cancer will give rise to aggressive disease that is refractory to treatment and so has poor prognosis (4). Indeed, elevated Hsp27 expression in tumors correlates with shorter disease-free survival and recurrence in node-negative breast cancer (10, 11), whereas the induction of Hsp27 following chemotherapy predicts poor prognosis and shorter disease-free survival (12). Currently, several selective Hsp27 inhibitors have reached clinical trials, including the Hsp27 inhibitor, OGX-427, which has completed phase I trials (clinicaltrials.gov - NCT00487786) and is now in phase II trials of castrate-resistant prostate cancer (clinicaltrials.gov - NCT01120470) and bladder cancer (clinicaltrials.gov - NCT00959868).

The inability of CD8$^+$ T cells to recognize tumor-associated antigenic (TAA) peptides presented on MHC class I molecules remains a formidable barrier, limiting the success of immunotherapy (13). In normal cells, the proteasome system efficiently generates peptides from intracellular antigens, which are loaded onto MHC class I molecules for presentation to T cells (14). Within the proteasome system,

Authors' Affiliations: [1]Division of Investigative Pathology, Scott & White Memorial Hospital and Clinic and the Texas A&M Health Science Center, College of Medicine, Temple, Texas; [2]Cell Biology Unit, Institut Pasteur de Montevideo, Montevideo, Uruguay; and [3]Department of Radiotherapy and Radiooncology, Technische Universität München and Helmholtz Center Munich, Clinical Cooperation Group (CCG) "Innate Immunity in Tumor Biology" Munich, Munich, Germany

Note: Supplementary data for this article are available at Cancer Prevention Research Online (http://cancerprevres.aacrjournals.org/).

Corresponding Author: Alexzander Asea, Chief, Division of Investigative Pathology, Scott & White Healthcare and the Texas A&M Health Science Center, College of Medicine, Temple, TX 76504. Phone: 1-254-743-0201; Fax: 1-254-743-0247; E-mail: asea@medicine.tamhsc.edu or aasea@swmail.sw.org

doi: 10.1158/1940-6207.CAPR-11-0121

Published OnlineFirst December 20, 2011; DOI:10.1158/1940-6207.CAPR-11-0121

the proteasome activator 28 (PA28) subunit, is a modulator of the proteasome-catalyzed generation of peptides presented via MHC class I molecules, and the selective increase in cellular levels of PA28α results in improved antigen presentation (15, 16). In addition, PA28 is essential for the recognition of epitopes on melanoma cells by specific cytotoxic T lymphocytes (CTL; ref. 17) and may alter the quality of products generated by proteasome cleavage (18, 19). The overexpression of the PA28α/β subunit enhanced MHC class I–restricted presentation of 2 viral epitopes and purified PA28α and PA28β subunit–accelerated T-cell epitope generation by the 20S proteasome *in vitro* (15). Taken together, these studies suggest that an efficient, well-functioning proteasome system is beneficial for specific $CD8^+$ CTL recognition of tumors and ultimately cytolysis (for review, see ref. 20).

In this study, we showed that short-term silencing of Hsp25 or Hsp27 using siRNA or permanent silencing of Hsp25 using lentivirus RNA interference technology enhanced proteasome activity via increased PA28α subunit expression, abrogated metastatic potential, induced the regression of established breast cancer cells via tumor-specific $CD8^+$ T cells, and stimulated long-lasting memory responses.

Materials and Methods

Cells and culture conditions

4T1 cells are a highly metastatic breast cancer cell line derived from a spontaneously arising BALB/c mammary tumor. BNL 1MEA.7R.1 (BNL) cells are a mouse-transformed hepatocellular carcinoma (HCC) cell line derived from BALB/c mice. MCF7 cells are a nonaggressive human breast cancer cell line. MDA-MB-232 cells are a highly aggressive human breast cancer cell line. All breast cancer cells were purchased directly from the American Type Cell Culture (ATCC), which routinely conducts cell line characterization. All breast cancer cells were passaged in our laboratory for not more than 6 months after receiving them from ATCC. 4T1 cells were maintained in monolayer cultures in Dulbecco's Modified Eagle's Medium (DMEM; Cellgro) supplemented with 10% FBS and antibiotics/antimycotics (Invitrogen Life Technologies). BNL cells were maintained in DMEM supplemented with 10% heat-inactivated FBS, antibiotics, and antimycotics (Gibco BRL/Life Technologies, Inc.). MCF7 cells were maintained in minimum essential medium (Eagle) with 2 mmol/L L-glutamine and Earle's balanced salt solution adjusted to contain 1.5 g/L sodium bicarbonate, 0.1 mmol/L nonessential amino acids, and 1 mmol/L sodium pyruvate and supplemented with 0.01 mg/mL bovine insulin and 10% FBS. MDA-MB-231 cells were maintained in ATCC-formulated Leibovitz L-15 medium supplemented with 10% heat-inactivated FBS, antibiotics, and antimycotics (Gibco BRL/Life Technologies, Inc.). All breast cancer cells were maintained in an incubator adjusted to 37°C with humidified atmosphere and 5% CO_2.

Preparation of small hairpin RNA from mouse Hsp25 using lentivirus gene transfer vector

An HIV-derived 3-plasmid system was kindly provided by D. Trono (Department of Microbiology and Molecular Medicine, University of Geneva, Geneva, Switzerland). The packaging plasmid psPAX2 encodes HIV-1 gag and pol genes. The envelope plasmid pMD2G encodes vesicular stomatitis virus (VSV) G envelope protein. The transfer vector pLVTHM encodes elongation factor-1α (*EF-1α*) and *H1* promoters, GFP as fluorescent marker, and woodchuck hepatitis posttranscriptional regulatory element (WPRE). The siRNAs for *hsp25* were designed using the standard web-based program (Invitrogen). The siRNAs were then converted into small hairpin RNA (shRNA) according to the web-based program from Promega. The shRNAs contained restriction overhangs such as *Mlu*I and *Cla*I and standard hairpin loop structure TTCAAGAGA and a Pol III termination signal which consists of a run of at least 4Ts (TTTTTT). Oligos were synthesized at the minimal synthesis and purification scales. Then, the complimentary oligos were annealed according to the manufacturer's instruction (Invitrogen). To construct vector plasmids, the plasmid pLVTHM was digested with *Mlu*I and *Cla*I and ligated to an oligonucleotide pair containing Hsp25shRNA or control shRNA carrying *Mlu*I and *Cla*I restriction overhangs and transformed into Max Stbl2 competent cells. The positive clones were identified by digesting the control pLVTHM vector and the vector containing Hsp25shRNA inserts using *Mlu*I and *Xba*I enzymes. Positive clones were also identified by DNA sequencing.

Lentivirus production and transduction

See supplementary information section.

Hsp25 and Hsp27 plasmids

See supplementary information section.

Animals and tumor challenge

See supplementary information section.

Live animal imaging

See supplementary information section.

Preparation of bone marrow–derived macrophages and *in vitro* cross-presentation assay

See supplementary information section.

In vivo antibody depletion assay

See supplementary information section.

Isolation and purification of $CD8^+$ and $CD8^-$ T cells for the *in vivo* adoptive transfer assay

See supplementary information section.

In vitro cytotoxicity assay

See supplementary information section.

Published OnlineFirst December 20, 2011; DOI:10.1158/1940-6207.CAPR-11-0121

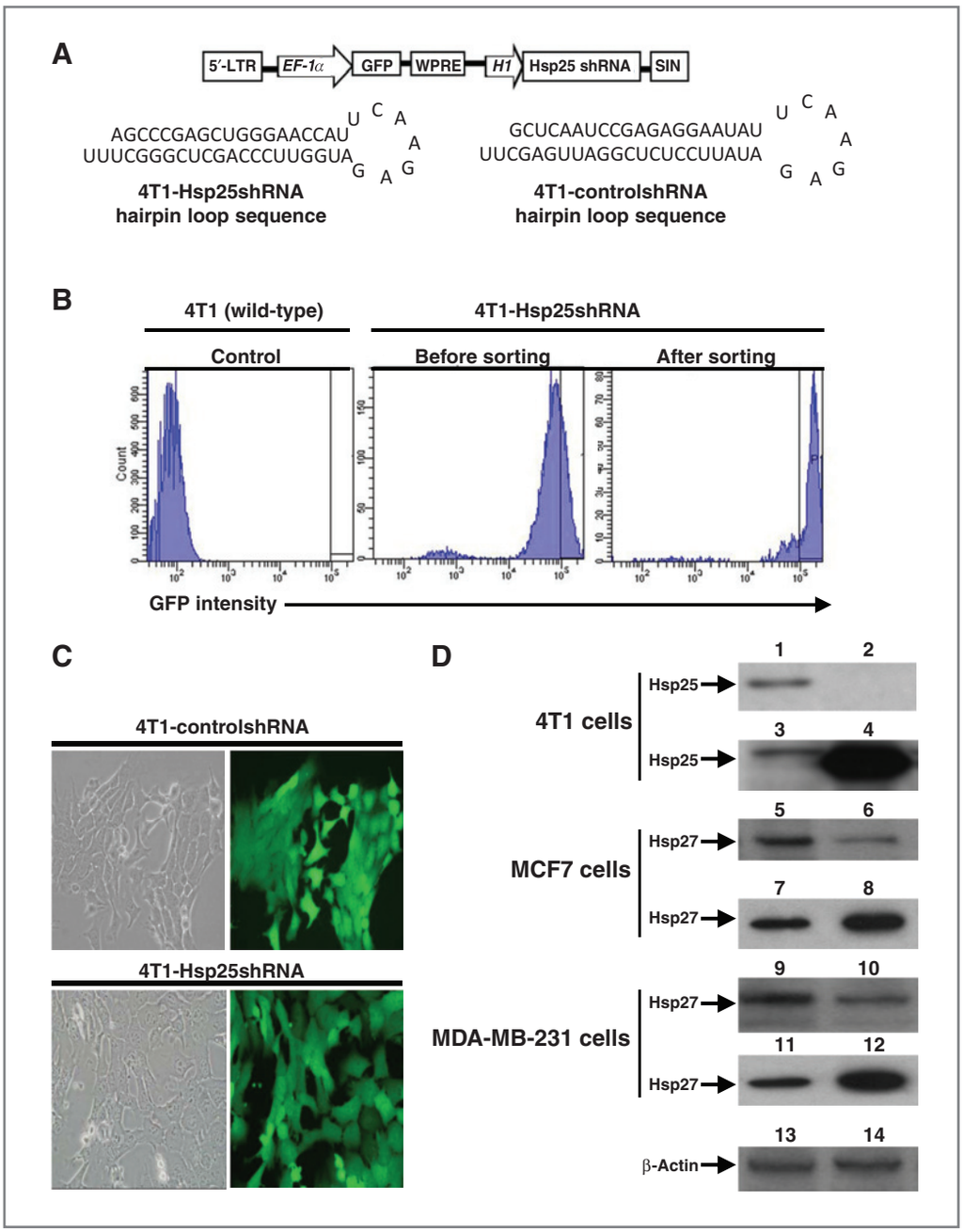

Figure 1. The expression of Hsp25 and Hsp27 in mouse and human breast cancer cells is effectively downregulated using Hsp25shRNA and Hsp25-siRNA respectively. A, HIV-based lentivirus construct pLVTHM was used to infect 4T1 cells. Construct contains a 5′-long terminal repeats (LTR), gene encoding GFP as reporter, and WPRE as enhancer of gene expression, placed under the tight control of *EF-1α* promoter. The Hsp25shRNA stem loop was placed downstream of the *H1* promoter, and the self-inactivating (SIN) element was placed downstream of the H1-Hsp25shRNA sequence (top). Schematic representation of 4T1-Hsp25shRNA and 4T1-controlshRNA hairpin sequences (bottom). B, FACSAria-generated histograms of lentivirus-infected 4T1 cells showing a relative number of cells (ordinate) and GFP intensity (abscissa) of gated 4T1-wt cells (left histogram), 4T1-Hsp25shRNA cells before sorting (middle), and after cell sorting (right). Data are representative of 3 independently carried out experiments with similar results. C, sorted 4T1-controlshRNA (top) or 4T1-Hsp25shRNA (bottom) cells were imaged using a digital inverted fluorescent microscope. Micropictograms are phase contrast (left) and fluorescent images (right) and were obtained under 40× magnification. Data are representative of 5 independently carried out experiments with similar results. D, 4T1-controlshRNA (lanes 1 and 13), 4T1-Hsp25shRNA (lanes 2 and 14), or 4T1 cells transfected with Ctrl-plasmid (lane 3) and Hsp25-plasmid (lane 4) for 72 hours at 37°C; or MCF7 cells transfected with Ctrl-siRNA (lane 5), Hsp27-siRNA (lane 6), Ctrl-plasmid (lane 7) and Hsp27-siRNA (lane 8) for 72 hours at 37°C; or MDA-MB-231 cells transfected with Ctrl-siRNA (lane 9), Hsp27-siRNA (lane 10), Ctrl-plasmid (lane 11), and Hsp27-siRNA (lane 12) for 72 hours at 37°C. Western blot analysis was conducted on protein lysates and immunoblotted with anti-Hsp25 or anti-Hsp27 or β-actin (as loading control). Data are representative of 3 independently carried out experiments with similar results.

Published OnlineFirst December 20, 2011; DOI:10.1158/1940-6207.CAPR-11-0121

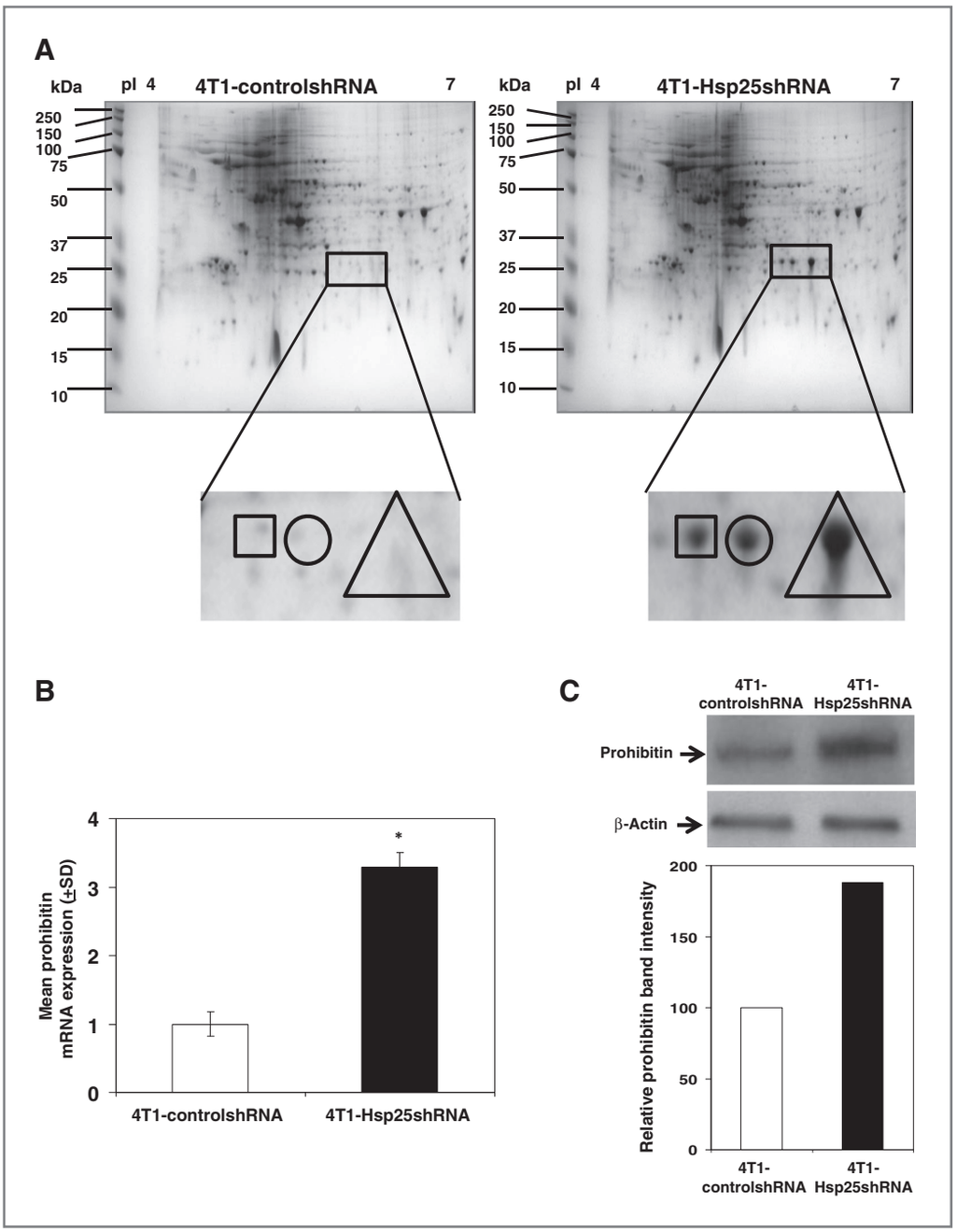

Figure 2. Silencing Hsp25 protein expression enhances prohibitin expression. A, proteins from 4T1-controlshRNA cells (left) or 4T1-Hsp25shRNA cells (right) were focused over an immobilized pH gradient of 4 to 7, separated on 8% to 16% SDS-PAGE gel and stained with Bio-Safe Coomassie. Protein spot found within the square (□) represents Ng,Ng-dimethylarginine dimethylaminohydrolase-2 and prohibitin; protein spot found within the circle (○) represents proteasome (prosome, macropain) 28 subunit alpha, PA28α and protein spot found within the triangle (Δ) represents undetectable proteins, as judged by mass spectrometry. Data are a representative experiment from 3 independently carried out experiments with similar results. B, 4T1-controlshRNA cells (open bar) and 4T1-Hsp25shRNA cells (filled bars) were used to isolate total RNA, and the relative prohibitin mRNA expression was measured using real-time PCR analysis. Data are the mean prohibitin mRNA expression (±SD) and are the sum of 3 independently carried out experiments. *, $P < 0.001$ vs. 4T1-controlshRNA cells (Student *t* test). C, 4T1-controlshRNA cells (left lanes) and 4T1-Hsp25shRNA cells (right lanes) were lysed, proteins extracted and subjected to immunoblotting with anti-prohibitin Mab (top) or β-actin (middle). The intensity of the bands were analyzed by densitometry with a video densitometer (ChemiImager 5500; Alpha Innotech) using the AAB software (American Applied Biology; bottom). Bars represent the mean prohibitin protein expression from 4T1-controlshRNA cells (open bar) and 4T1-Hsp25shRNA cells (filled bar) and are a representative experiment from 3 independently carried out experiments with similar results.

Published OnlineFirst December 20, 2011; DOI:10.1158/1940-6207.CAPR-11-0121

Table 1. Identification of unique proteins in lentivirus-mediated Hsp25 knockdown in 4T1 cells using mass spectrometry

2D-Gel spot[a]	Protein name	Database accession number	Distinct summed MS/MS search score	Protein molecular weight (kDa)/pI	% amino acid coverage	Number of peptides
Square	Ng,Ng-dimethylarginine dimethylaminohydrolase-2	45476968	81.94	29,646/5.66	27	5
	Prohibitin	74181431	65.46	29,850/5.40	21	5
Circle	Proteasome (prosome, macropain) 28 subunit-alpha, PA28α	12842740	168.86	28,640/5.48	50	11
	Proteasome activator subunit 3	6755214	80.66	29,506/5.69	34	6
	Mitochondrial ribosomal protein L46	12963643	62.77	32,131/6.93	16	5
Triangle	Not detectable	—	—	—	—	—

[a]4T1-Hsp25shRNA cells were run on 2D-SDS-PAGE, and protein spot was excised using Bio-Rad's ExQuest spot cutter. Protein sample was digested in-gel, and peptides extracted and samples injected into an 1100 series HPLC-Chip cube MS interface, and Agilent 6300 series Ion Trap Chip-LC-MS/MS system (Agilent Technologies). The system is equipped with an HPLC-Chip (Agilent Technologies) that incorporates a 40-nL enrichment column and a 43 mm × 75 mm analytic column packed with Zorbex 300SB-C18 5-mm particles. Tandem MS spectra were searched against the National Center for Biological information nonredundant (NCBInr) mouse protein database, using Spectrum Mill Proteomics Work Bench for protein identification.

Proteasome activity assay

See supplementary information section.

Statistical analysis

For comparisons between groups, Dunn multiple comparison tests and the Student *t* test and one-way ANOVA were used in this study ($P < 0.001$ was considered significant).

Results

Permanent and transient silencing of *hsp25* or *hsp27* gene results in effective downregulation of Hsp25 and Hsp27 protein expression in mouse and human breast cancer cells

We used a lentivirus-based vector (pLVTHM) that expresses RNA interference inducing the 25-kDa Hsp25 shRNA (Hsp25shRNA) under the control of the *H1* promoter (Fig. 1A). This bicistronic vector was engineered to coexpress enhanced *GFP* (eGFP) as a reporter gene under the tight control of the *EF-1α*) promoter, permitting transduced/infected target cells to be tracked using *in vivo* imaging. Stable silencing of *hsp25* gene expression in 4T1 tumor cells was achieved by subcloning the Hsp25shRNA cassette into pLVTHM, a self-inactivating (SIN) lentiviral vector using *Mlu*I and *Cla*I restriction sites (4T1-Hsp25shRNA hairpin loop sequence; Fig. 1A). We also constructed control/scrambled shRNA-containing lentiviral vector which does not have sequence homology to the mouse genome (4T1-controlshRNA hairpin loop sequence; Fig. 1A). These constructs were introduced into 293FT viral packaging cells to make lentivirus. The concentrated lentivirus preparation was used to infect target 4T1 breast adenocarcinoma cells. The resulting GFP expression was assessed 4 days postinfection by flow cytometry and further enriched for only highly expressing GFP-positive cells. The resulting sorted 4T1-Hsp25shRNA cells were 96.7% positive for GFP (Fig. 1B). The high GFP expression exhibited by both 4T1-controlshRNA and Hsp25shRNA stably transfected cells remained high even after 6 weeks of culture (Fig. 1C). We confirmed that high GFP expression in 4T1-Hsp25shRNA cells corresponded to efficient silencing of Hsp25 protein expression consistently by more than 98% after 6 to 8 weeks *in vitro* cell culture, as compared with the expression of Hsp25 in 4T1-controlshRNA cells (Fig. 1D). To negate the possibility that the stable transfection of only one cell line with Hsp25shRNA and selection after 6 to 8 weeks of culture might lead to the selection of a particular phenotype, additional experiments after short-term treatment with siRNA were also carried out. We showed that transient transfection of human breast cancer cells MCF7 and MDA-MB-231 with Hsp27-siRNA resulted in effective suppression of Hsp27 protein expression as compared with cells transfected with control-siRNA (Ctrl-siRNA; Fig. 1D). Gain-of-function experiments using Hsp25-plasmids in 4T1 cells and Hsp27-plasmids in MCF7 cells and MDA-MB-231 cells resulted in the significant increase in Hsp25 and Hsp27 expression, as compared with control-plasmid (Ctrl-plasmid; Fig. 1D).

Silencing Hsp25 increases cell death in tumor cells and increases the tumors ability to migrate *in vitro*

The uncontrollable growth of tumors and their ability to metastasize and invade distant organs is the hallmark of aggressive forms of cancer. We showed that silencing Hsp25 protein expression dramatically increased cell death in tumor cells and the ability of the tumor to migrate *in vitro*. There were consistently lesser cells recovered from culture plates of 4T1-Hsp25shRNA cells as than 4T1-controlshRNA

Published OnlineFirst December 20, 2011; DOI:10.1158/1940-6207.CAPR-11-0121

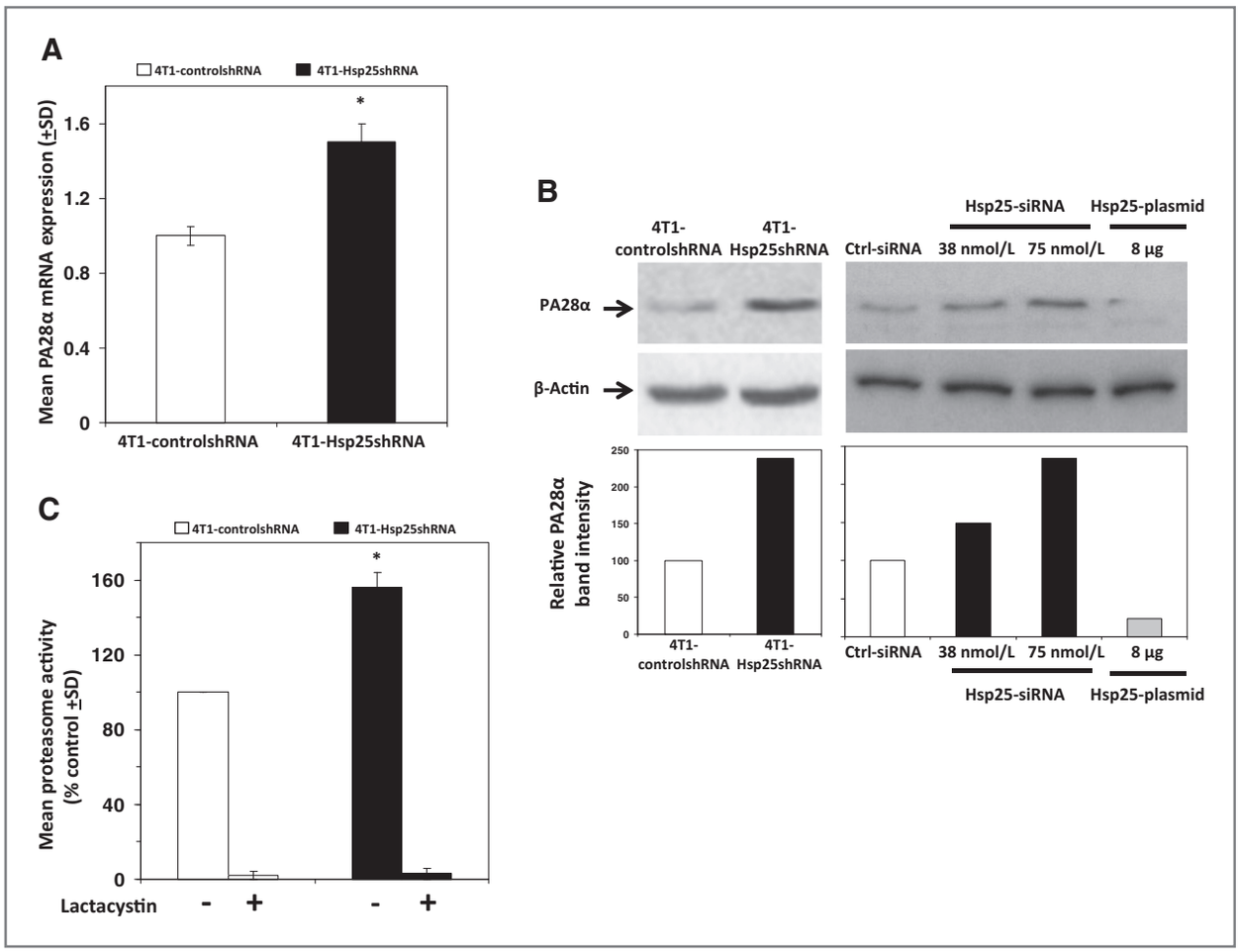

Figure 3. Silencing Hsp25/27 expression enhances proteasome activity and the expression of proteins associated with cell death and antigen presentation and suppresses the expression of proteins associated with cancer and cell movement. A, 4T1-controlshRNA cells (open bars) and 4T1-Hsp25shRNA cells (filled bars) were used to isolate total RNA, and the relative PA28α mRNA expression was measured using real-time PCR analysis. Bars are the mean PA28α mRNA expression (±SD) and are the sum of 4 independently carried out experiments. *, $P < 0.001$ vs. 4T1-controlshRNA cells (Student *t* test). B, 4T1-controlshRNA cells (left, lane 1), 4T1-Hsp25shRNA cells (left, lane 2), 4T1-wt cells were transfected with Ctrl-siRNA (right, lane 1), 38 nmol/L Hsp25-siRNA (right, lane 2), 75 nmol/L Hsp25-siRNA (right, lane 3), or 8 μg Hsp25-plasmid (lane 4), for 72 hours at 37°C. Cells were then lysed and proteins extracted and subjected to immunoblotting with anti-PA28α Mab (top) or β-actin (middle). The intensity of the bands were analyzed by densitometry with a video densitometer (Chemilmager 5500; Alpha Innotech) using the AAB software (bottom). Bars represent the relative PA28α band intensity and are a representative experiment from 3 independently carried out experiments with similar results. C, the 20S proteasome activity was measured by incubation of cell extracts from 30 μg 4T1-controlshRNA (open bars) or 4T1-Hsp25shRNA (filled bars) for 90 minutes with a fluorogenic substrate (Suc-LLVY-AMC) in the absence or presence of lactacystin (25 μmol/L). Free AMC fluorescence was measured by using a 380/460 nm filter set in a fluorometer. Data are the mean proteasome activity (% control ± SD) and are the sum of 3 independently carried out experiments. *, $P < 0.001$ vs. 4T1-controlshRNA cells (Student *t* test).

or wild-type 4T1 (4T1-wt) cells (Supplementary Fig. S1A, left). Results of cell death measurements suggest the low cell count is due to a concomitant increase in the percentage of cell death in 4T1-Hsp25shRNA cells as compared with 4T1-controlshRNA or 4T1-wt (Supplementary Fig. S1A, right). We showed that Hsp25shRNA treatment adversely affects the directional cell migration of 4T1 cells *in vitro*, approximately to the same extent as serum starvation, as judged by the wound-healing experiment (Supplementary Fig. S1B). These results correlated well with the inability of 4T1-Hsp25shRNA cells to invade extracellular matrix *in vitro* as compared with 4T1-controlshRNA cells (Supplementary Fig. S1C).

We validated these data in experiments in which mouse and human breast cancer cells were transiently transfected with siRNA directed against Hsp25 or Hsp27, respectively. We showed that silencing Hsp25/27 effectively suppressed the expression of proteins known to be important in cancer functions including; ABCB4 (growth, survival, proliferation), ENO1 (growth, differentiation, colony formation), HSP90AB1 (survival, migration, negative regulation of proteasomal ubiquitin-dependent protein catabolic process), HSPA8 (apoptosis, ubiquitination, cell-cycle progression, survival, cell viability), lactate dehydrogenase (LDH; growth, transformation, proliferation), MCM3 (growth, migration), and MIF (proliferation,

Published OnlineFirst December 20, 2011; DOI:10.1158/1940-6207.CAPR-11-0121

Table 2. Modulation of proteasome activity in mouse and human breast cancer cells by silencing and overexpression of *hsp25* and *hsp27* genes, respectively

		Mean percentage proteasome activity as compared with respective control (% control ± SD)[c]		
Cells[a]	Treatment[b]	Total[d]	Caspase-like[e]	Trypsin-like[f]
4T1 cells	Hsp25-siRNA	52 ± 5[g]	25 ± 4[g]	22 ± 7[g]
4T1 cells	Hsp25-plasmid	−15 ± 5[g]	−102 ± 9[g]	ND
MDA-MB-231 cells	Hsp27-siRNA	48 ± 12[g]	128 ± 15[g]	78 ± 25[g]
MDA-MB-231 cells	Hsp27-plasmid	−21 ± 5[g]	−75 ± 8[g]	−53 ± 6[g]
MCF7 cells	Hsp27-siRNA	32 ± 10[g]	202 ± 20[g]	12 ± 3[g]
MCF7 cells	Hsp27-plasmid	−15 ± 5[g]	−66 ± 10[g]	−32 ± 9[g]

[a]Mouse (4T1) or human (MDA-MB-231 or MCF7) breast cancer cells (5,000 cells) were plated in 100 μL complete culture media in a 96-well plate overnight in a 37°C incubator.
[b]Cells were transfected with 75 nmol/L Hsp25-siRNA (Qiagen) or 15 nmol/L Hsp27-siRNA (Qiagen) or 8 μg Hsp25/Hsp27-plasmids (Origene) using Lipofectamine RNAiMAX and Lipofectamine 2000 (Invitrogen) and incubated for a further 72 hours in a 37°C incubator.
[c]The mean percentage proteasome activity as compared with respective control (% control ± SD) is the sum of 3 independently carried out experiments.
[d]Total proteasome activity was measured using the 20S Proteasome Activity Assay Kit (Millipore) against the fluorogenic proteasome substrate, Suc-LLVY-AMC according to the manufacturer's instructions (Millipore).
[e]Caspase-like proteasome activity was measured using the Proteasome-Glo Caspase-like Kit (Promega) according to the manufacturer's instructions (Promega). Luminescence was measured with an EG&G Berthold microplate luminometer.
[f]Trypsin-like proteasome activity was measured using the Proteasome-Glo Trypsin-like Kit (Promega) according to the manufacturer's instructions (Promega). Luminescence was measured with an EG&G Berthold microplate luminometer.
[g]$P < 0.001$ vs. control (Student *t* test).

activation, migration). In addition, there was a concomitant decrease in the expression of proteins associated with cell movement [e.g., CAP (morphogenesis, migration, organization, morphology, depolymerization, elongation), EMTH (proliferation, quantity, development, activation), FLNA (cell spreading, motility, formation, migration), FLNB (migration, binding, anchoring), HSPD1 (chemotaxis, polarity, migration), MYH9 (adhesion, morphogenesis, movement, retraction, migration, formation), S100A6 (proliferation, survival, invasion, focus formation), and TWIST1 (survival, migration, motility, adhesion, proliferation]. On the other hand, there was an increase in the expression of proteins known to be associated with cell death [e.g., EEF2 (autophagy, cell death, apoptosis), FASN (apoptosis, G_1 phase, G_2 phase, senescence), GAPDH (apoptosis, cell death, caspase-independent cell death), HNRNPA1 (apoptosis, nuclear export, alternative splicing, stress response), KRT18 (apoptosis, cell death, collapse, fragmentation), YWHAE (apoptosis, cell-cycle progression, mitosis, transmembrane potential)] and antigen presentation [e.g., PSMB5 (degradation, proteolysis), TAP1 (autophosphorylation, antigen presentation), TAPBP (substrate selection, ubiquitination, selection, immune response); Supplementary Fig. S1D]. Together, these results indicate that silencing the expression of Hsp25/27 in breast adenocarcinoma tumors significantly interferes with its ability to survive and migrate *in vitro*.

Hsp25/27 expression modulates proteasome activity in breast cancer cells

To obtain an integrative understanding of the effect of Hsp25 silencing on the global protein profile of 4T1 breast adenocarcinoma cells, we used 2-dimensional (2D) SDS-PAGE combined with liquid chromatography/tandem mass spectrometry (LC/MS-MS) techniques to compare the protein profiles between controlshRNA and Hsp25shRNA stably transfected 4T1 cells. Three unique spots were selected from 4T1-Hsp25shRNA cells (Fig. 2A, right) which were absent in 4T1-controlshRNA cells (Fig. 2A, left). Further characterization using LC/MS-MS and bioinformatics revealed that the unique proteins were Ng,Ng-dimethylarginine dimethylaminohydrolase-2 and prohibitin (Table 1, square), PA28α, PA28γ subunits, and mitochondrial ribosomal protein L46 (Table 1, circle). Proteins expressed within the triangle could not be identified, possibly due to the highly glycosidic nature of the proteins (Table 1, triangle). Because of the obvious relevance to tumor growth and metastasis, we chose to validate prohibitin and PA28α by real-time PCR and Western blot analysis. We showed that silencing the *hsp25* gene increased prohibitin mRNA expression by 3-fold (Fig. 2B). The mRNA expression levels correlated well with a 2.5-fold increase in prohibitin protein expression as judged by Western blot analysis (Fig. 2C). Similar increases were observed for PA28α mRNA expression which was upregulated by 1.5-fold, as judged by real-time PCR (Fig. 3A) and by 2-fold as judged by Western blot

Published OnlineFirst December 20, 2011; DOI:10.1158/1940-6207.CAPR-11-0121

analysis (Fig. 3B, left), as compared with respective controls. There was no significant alteration in the PA28γ subunit by measuring protein and RNA levels (data not shown). Transient transfection experiments showed that treatment of 4T1 cells transfected with Hsp25-siRNA dose dependently increased PA28α expression (Fig. 3B). Gain-of-function experiments to increase Hsp25 expression in 4T1 cells (using Hsp25-plasmids) showed that the overexpression of Hsp25 dramatically suppresses PA28α expression (Fig. 3B). To further validate the finding that silencing Hsp25 protein expression increases proteasome activity, we measured the chymotrypsin-like activity of 20S proteasome in 4T1-controlshRNA and 4T1-Hsp25shRNA cell extracts. We showed that 4T1-Hsp25shRNA cells showed 50% greater proteasome activity than 4T1-controlshRNA tumor cells (Fig. 3C). Because chymotrypsin-like activity of 20S proteasome uses Suc-LLVY-AMC as the substrate for proteasome activity measurement, we also measured trypsin-like and caspase-like proteasome activities in mouse and human breast cancer cells. We showed that transient transfection using Hsp25-siRNA and Hsp27-siRNA effectively increases chymotrypsin-like, caspase-like, and trypsin-like proteasome activities in 4T1, MCF7, and MDA-MD-231 cells, as compared with respective control-siRNA's (Ctrl-siRNA; Table 2). The overexpression of Hsp25 and Hsp27 (using Hsp25-plasmid and Hsp27-plasmid, respectively) suppressed chymotrypsin-like, caspase-like, and trypsin-like proteasome activities in 4T1, MCF7, and MDA-MD-231 cells, as compared with respective control plasmids (Ctrl-plasmids; Table 2). Taken together, these results indicate that silencing of Hsp25 or Hsp27 enhances proteasome function *via* PA28α.

Silencing Hsp25/27 expression induces tumor regression and inhibits metastasis

To determine the consequence of lentivirus-mediated *hsp25* gene silencing *in vivo*, 4T1-controlshRNA and 4T1-Hsp25shRNA cells were injected subcutaneously into the mammary pad of female BALB/c mice. As early as 7 days after tumor cells injection (TCI), tumors could be visualized growing in the mammary pad of all mice using the Maestro *In Vivo* Imaging System (CRI). We showed that 13 days post-TCI, the GFP signal from 4T1-controlshRNA tumors were significantly higher than GFP signal from 4T1-Hsp25shRNA tumors (Fig. 4A). Starting 7 days post-TCI, there was a steady regression in GFP signal from 4T1-Hsp25shRNA tumors. By day 25 post-TCI, there was no detectable GFP signal in any mouse bearing 4T1-Hsp25shRNA tumors (Fig. 4A). Efficient Hsp25 silencing (>95%) could still be shown in 4T1-Hsp25shRNA tumors before they completely disappeared (data not shown). To negate the possibility that antitumor responses were directed against the GFP protein instead of unknown "tumor-associated antigens" that are better processed as a consequence of silencing Hsp25 expression in tumor cells, tumor growth experiments using eGFP positive (+) and negative(−) 4T1-Hsp25shRNA and 4T1-controlshRNA and wild-type 4T1 cells were carried out. We showed that eGFP did not significantly alter tumor growth curves of BALB/c wild-type mice injected with eGFP positive (+) or negative(−) 4T1-controlshRNA cells (Fig. 4B, left). Experiments carried out in BALB/c nude mice further revealed that the tumor volume of 4T1-Hsp25shRNA cells (with or without GFP) is significantly smaller than 4T1-controlshRNA (with or without GFP) or 4T1-wt cells (Fig. 4B, right). An additional observation observed in the BALB/c nude mice experiments was that whereas the injected 4T1-controlshRNA and 4T1-wt cells rapidly metastasize to distant organs including lungs, liver, and brain, injected 4T1-Hsp25shRNA cells did not metastasize to these organs (data not shown), suggesting that although a competent immune system (possibly $CD8^+$ CTL) may be one of the mechanisms associated with downregulation of Hsp25, there might be other mechanisms. At the end of the experiment (day 34 post-TCI), gross pathology of multiple organs, including lungs, brain, bone and liver, showed an absence of tumor metastasis in mice injected with 4T1-Hsp25shRNA but not 4T1-controlshRNA mice. Hematoxylin and eosin staining of lungs from mice injected with 4T1-controlshRNA revealed micrometastasis in lung tissues (Fig. 4C, left). In contrast, lungs of mice injected with 4T1-Hsp25shRNA had no visible micrometastasis (Fig. 4C, right). To confirm that micrometastasis undetectable by light microscopy did not exist in 4T1-Hsp25shRNA–injected mice, we conducted clonogenicity assays on lung tissues in complete media containing 6-thioguanine. 4T1 breast adenocarcinoma cells are resistant to 6-thioguanine; however, all other contaminating cells will be destroyed. Mice injected with the 4T1-controlshRNA cells exhibited large numbers of colonies at all dilutions, reflecting robust metastasis of tumors to the lungs (Fig. 4D). In contrast, no colonies were observed in dishes plated with lung tissue harvested from mice injected with 4T1-Hsp25shRNA cells (Fig. 4D). Taken together, these data suggest that permanent silencing of Hsp25 results in tumor regression and inhibition of metastasis *in vivo*.

Silencing Hsp25/27 activates specific $CD8^+$ CTL-killing functions and memory

To determine the nature of the cells responsible for tumor regression following silencing of Hsp25 expression in 4T1 breast adenocarcinoma cells, prior to TCI, we conducted *in vivo* depletion of cells known to play an important role in tumor regression. Here, we showed that *in vivo* depletion of $CD8^+$ CTL prior to injection of 4T1-controlshRNA cells drastically increased tumor growth rate, and by day 34 post-TCI, the size of the tumors were approximately 10 times larger than mice injected with PBS only (Fig. 5A, left). The *in vivo* depletion of $CD4^+$ T cells did not significantly alter tumor growth rate or tumor volume in mice injected with 4T1-controlshRNA cells (Fig. 5A, left). Unexpectedly, using similar mice, the *in vivo* depletion of natural killer (NK) cells using the 5E6 monoclonal antibody induced complete tumor regression (Fig. 5A, left). In mice injected with 4T1-Hsp25shRNA cells, no tumor growth was seen in any of the mice by the end of the experiment (Fig. 5A, right). As expected, the *in vivo* depletion of $CD8^+$ T cells and NK cells

Published OnlineFirst December 20, 2011; DOI:10.1158/1940-6207.CAPR-11-0121

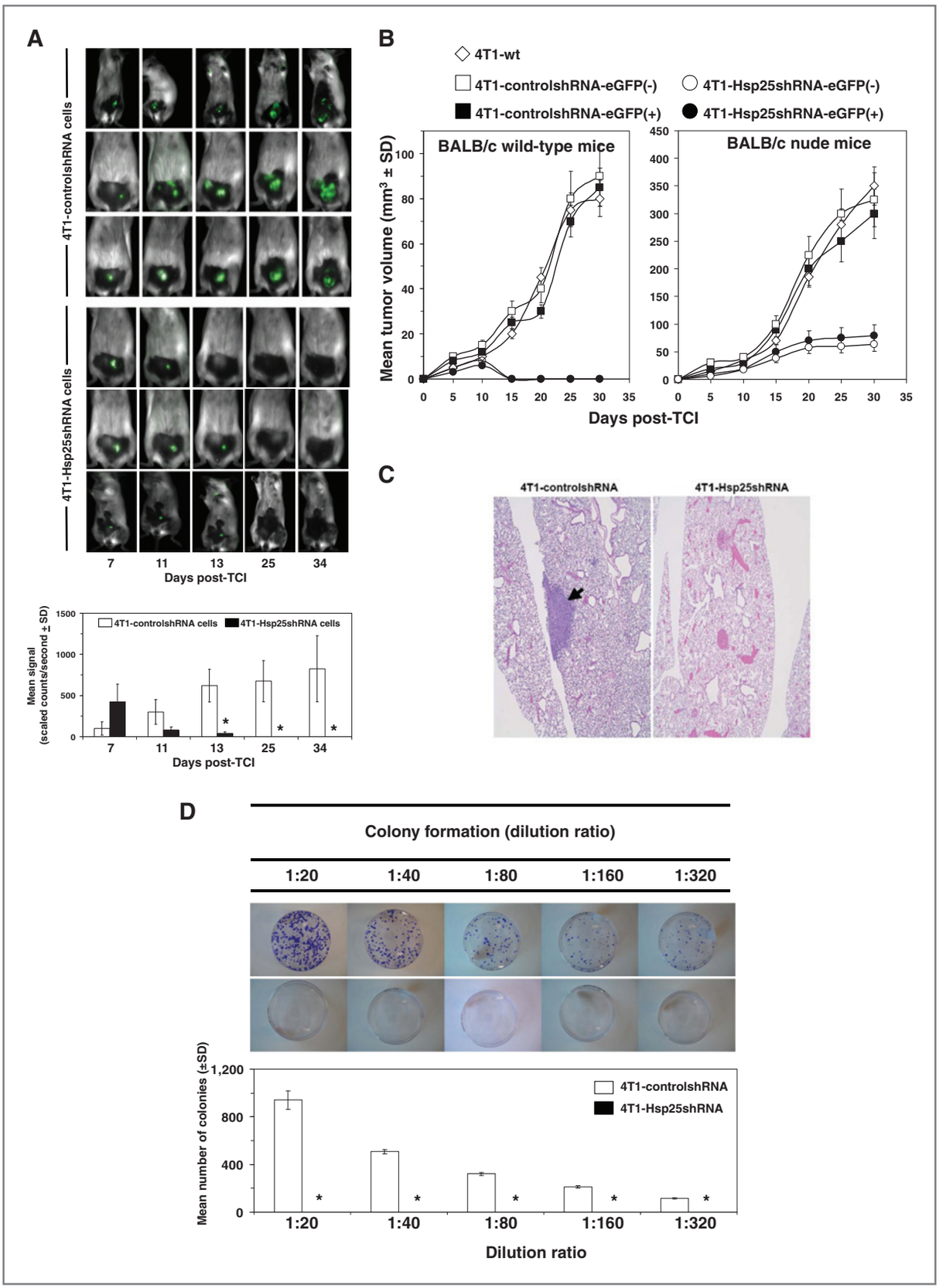

Published OnlineFirst December 20, 2011; DOI:10.1158/1940-6207.CAPR-11-0121

prior to injection with 4T1-Hsp25shRNA cells resulted in tumor growth. Similar depletion of $CD4^+$ T cells initially resulted in increased tumor growth, followed by tumor regression (Fig. 5A, right). Interestingly, the *in vivo* depletion of $CD8^+$ T cells prior to injection with 4T1-Hsp25shRNA cells resulted in increased tumor growth (Fig. 5A, right). Gross pathology of lung, brain, and bone did not reveal any signs of metastasis to the lungs (data not shown). Similarly, injection of 4T1-Hsp25shRNA cells into the breast pad of BALB/c nude mice resulted in tumor growth without metastasis (data not shown).

To confirm that $CD8^+$ T cells mediated the enhanced cytolytic effects after silencing Hsp25, reactive $CD8^+$ T cells were harvested from the spleen of mice which had been injected with 4T1-Hsp25shRNA cells and were tumor free (days 21–28 post-TCI) and the specific T-cell cytotoxicity measured against 4T1-controlRNA target cells *ex vivo*. Extracted splenic $CD8^+$ T cells were enriched using negative selection by magnetic beads and consistently exhibited greater than 95% purity, as judged by flow cytometry (Fig. 5B). Experiments were next carried out to negate the possibility that the tumor-associated response was directed against GFP protein. We showed that reactive $CD8^+$ T, but not $CD8^-$ T cells (non-$CD8^+$ T cells), effector cells harvested from the spleen of mice injected with 4T1-Hsp25shRNA cells exhibited potent-specific lysis against 4T1-controlshRNA eGFP-positive and eGFP-negative targets with similar activity (Fig. 5C). $CD8^+$ cells did not exhibit significant lytic activity against BNL, which served as an irrelevant target (Fig. 5C). As expected, both $CD8^+$ and $CD8^-$ T cells from mice injected with 4T1-controlshRNA cells did not mediate significant lysis above baseline levels against 4T1-controlshRNA targets.

To determine whether 4T1-Hsp25shRNA–reactive $CD8^+$ T cells can rescue mice injected with 4T1-controlshRNA cells, 4T1-Hsp25shRNA–reactive $CD8^+$ T cells were adoptively transferred into 4T1-controlshRNA tumor–bearing mice. As predicted, the adoptive transfer of 4T1-Hsp25shRNA–reactive $CD8^+$ T cells into 4T1-controlshRNA tumor–bearing mice induced significant tumor regression starting by day 17 post-TCI, and by day 28, there was no detectable tumor growth (Fig. 5D). In contrast, 4T1-controlshRNA tumor–bearing mice adoptively transferred with $CD8^-$ T-cell fraction were not protected and mice rapidly developed tumors (Fig. 5D) and metastasis (data not shown).

To prove that the improvement in antigen presentation is due, in part, to silencing of Hsp25 expression, we used the *in vitro* cross-presentation assay. Bone marrow-derived dendritic cells (BMDC) were recovered from female C57BL/6 ($H2^b$) and BALB/c ($H2^d$) mice and treated with ovalbumin (OVA) during the culture process. BMDCs were then transfected with either Hsp25-siRNA or negative control-siRNA and fixed with paraformaldehyde and later admixed with S8L peptide–specific T-cell hybridoma, B3Z cells. We showed that B3Z cells released significantly more IFN-γ when admixed with C57BL/6 ($H2^b$)-derived BMDCs in which Hsp25 has been silenced (Hsp25-siRNA) than control-siRNA–treated BMDCs (Fig. 5E; left). In addition, we showed that pretreatment of both Hsp25-siRNA–and control-siRNA–treated BMDCs with the specific proteasome inhibitor, MG-132, significantly reduced the concentration of released IFN-γ (Fig. 5E, left). Finally, we showed that BMDCs recovered from BALB/c mice which express $H2^d$ did not release significant quantities of IFN-γ under similar conditions (Fig. 5E; right). To prove that 4T1-Hsp25shRNA generates memory responses, tumor-free immunocompetent female BALB/c mice were rechallenged with wild-type 4T1 (4T1-wt) or an irrelevant tumor, murine transformed HCC cells, BNL, 60 days after initial challenge with 4T1-Hsp25shRNA. We showed that rechallenge of 4T1-wt cells does not result in tumor growth, which is similar to mice injected with 4T1-Hsp25shRNA alone (Fig. 5F). However, rechallenge with BNL (after 4T1-Hsp25shRNA) resulted in tumor growth in a similar fashion to mice injected with BNL alone (Fig. 5F).

Discussion

Mouse and human breast cancer cells express elevated levels of Hsp25 or Hsp27, respectively, which is effectively suppressed by permanently silencing Hsp25 or short-term silencing of Hsp25 and Hsp27 protein expression (Fig. 1D). This is important not only because elevated levels of Hsp27 in breast cancer give rise to aggressive disease and poor prognosis (4) but also because

Figure 4. Silencing *hsp25* gene expression in 4T1 cells induces tumor regression and metastasis *in vivo*. A, 4T1-controlshRNA cells or 4T1-Hsp25shRNA cells were injected into the mammary pads of female BALB/c mice, and tumor growth was monitored on specific days post-TCI using the Maestro *In Vivo* Imaging System (CRI). Data are fluorescent micropictograms of GFP-tagged tumors (green fluorescence) measured on various days post-TCI (top). Bars represent the mean GFP signal/exposure (total signal scaled counts/seconds ± SD) from 4T1-controlshRNA cells (open bars) or 4T1-Hsp25shRNA cells (filled bars) and are the sum of 3 mice per group ($n = 3$). *, $P < 0.001$ vs. 4T1-controlshRNA cells (Student *t* test; bottom). B, about 10^4 4T1-wt cells (open diamonds) or 4T1-controlshRNA-eGFP(−) cells (open squares) or 4T1-controlshRNA-eGFP(+) cells (filled squares) or 4T1-Hsp25shRNA-eGFP(−) cells (open circles) or 4T1-Hsp25RNA-eGFP(+) cells (filled circles) were injected into the mammary pads of female BALB/c wild-type mice (left) or female BALB/c nude mice (right), and tumor growth was monitored on specific days post-TCI using an electronic caliper. Data are mean tumor volume (mm^3 ± SD) and are a representative experiment from 2 independently carried out experiments ($n = 5$). C, hematoxylin and eosin staining of lungs from mice implanted with 4T1-controlshRNA cells (left) or 4T1-Hsp25RNA cells (right) 34 days after TCI into the breast pad (arrow indicates lung micrometastasis). Data are a representative of 4 independently carried out experiments with similar results. D, colony formation of tumors derived from lungs of mice injected with 4T1-controlshRNA (top) or 4T1-Hsp25shRNA cells (middle) into the breast pad. Homogenized lung tissue was platted at different dilution ratios (1:20–1:320). Plates were stained and the mean number of colonies was counted after staining with crystal violet. Bars represent the mean number of colonies (±SD) from lungs of mice implanted with 4T1-controlshRNA cells (open bars) or 4T1-Hsp25shRNA cells (filled bars) and are a representative experiment from 4 independently carried out experiments (bottom). *, $P < 0.001$ vs. 4T1-controlshRNA cells (Student *t* test).

Published OnlineFirst December 20, 2011; DOI:10.1158/1940-6207.CAPR-11-0121

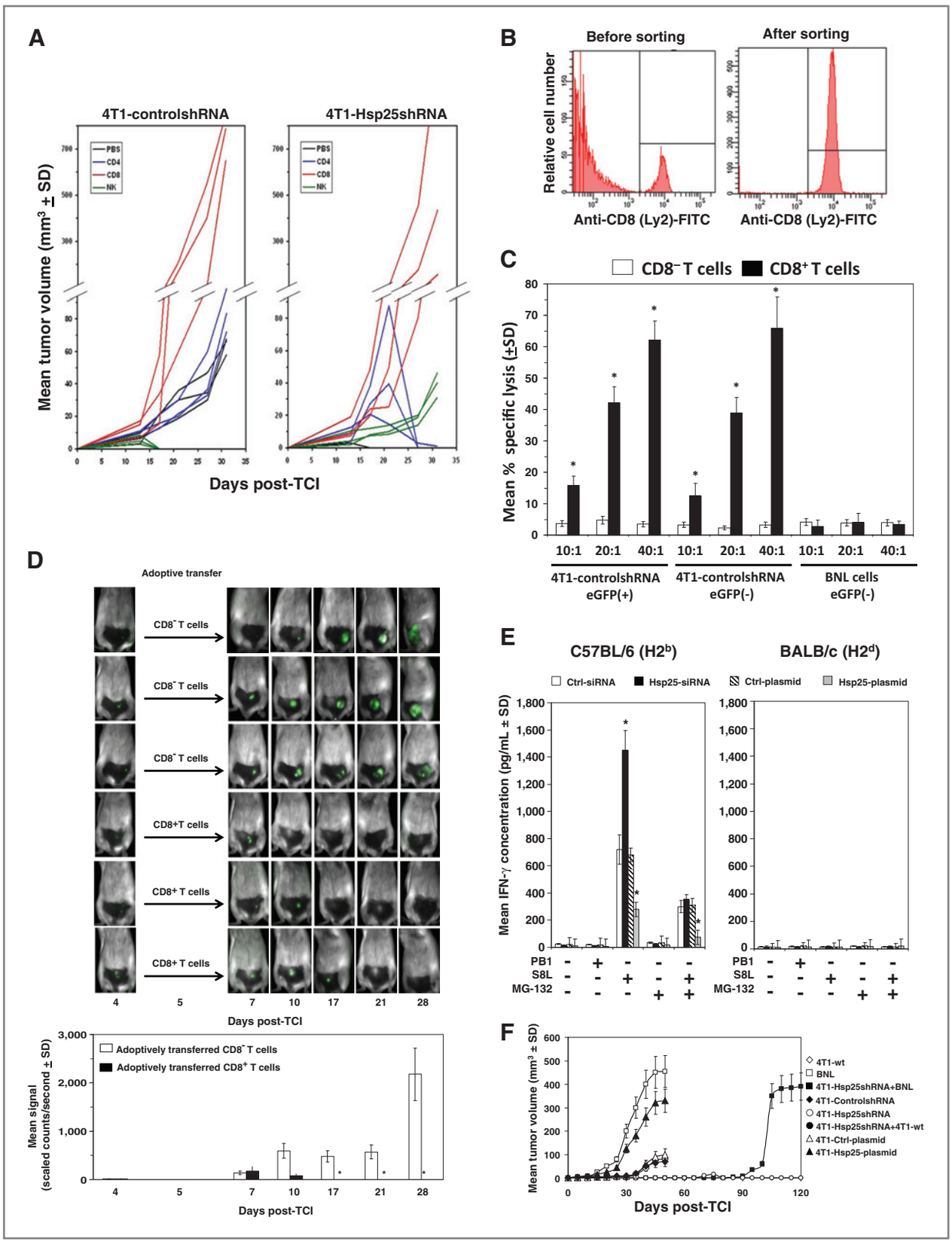

Published OnlineFirst December 20, 2011; DOI:10.1158/1940-6207.CAPR-11-0121

elevated Hsp27 levels have been reported to confer tumor protection against bortezomib-induced cell death (21). Bortezomib is characterized as a reversible proteasome inhibitor, with potent anticancer effects against multiple myeloma (22). Bortezomib was shown to effectively induce apoptotic cell death in DHL6 lymphoma cells (do not express significant Hsp27) but not in DHL4 lymphoma cells (expressing high basal levels of Hsp27). Blocking the elevated Hsp27 expression in DHL4 lymphoma cells using antisense against Hsp27 restored sensitivity to bortezomib. These authors concluded that combining agents that suppress Hsp27 expression might provide a therapeutic advantage to overcome tumors that might be resistant to bortezomib treatment (21).

Our study shows that silencing Hsp25/27 effectively suppresses proteins known to be important in cancer functions in cells (Supplementary Fig. S1D). Because the working hypothesis for this study is that high Hsp25/27 expression represses proteasome activity, therefore gain-of-function studies were also conducted. Our results showed that increasing Hsp25 or Hsp27 expression using Hsp25- or Hsp27-plasmids effectively increases Hsp25 or Hsp27 expression, respectively (Fig. 1D). The biologic significance of increased Hsp25 or Hsp27 expression was a significant increase in dramatic inhibition of PA28α protein expression (Fig. 3B). We further showed that silencing Hsp25 or Hsp27 concomitantly increases proteasome chymotrypsin-like activity (Fig. 3C). Because chymotrypsin-like activity uses Suc-LLVY-AMC as the substrate for proteasome activity measurement and because the same substrate can be digested by calpains, we also measured trypsin-like and caspase-like proteasome activities. We showed that knockdown of Hsp25 or Hsp27 expression enhanced chymotrypsin-like proteasome activity, caspase-like proteasome activity, and trypsin-like proteasome activity in mouse and human breast cancer cell lines, respectively (Table 2). This is significant because Groettrup and colleagues reported that increased expression of PA28α results in marked enhancement of recognition by virus-specific cytotoxic T cells (15). In addition, an essential role for PA28 was described in the melanoma cell line, Mel-18a. These authors showed that recognition of TRP2-expressing melanoma cells by $TRP2_{360–368}$–specific CTLs directly correlated with the presence of PA28, and impaired epitope presentation on Mel-18a cells could be rescued by transfection of PA28-encoding plasmids (17). Here, we showed that IFN-γ release from B3Z (an S8L peptide–specific T-cell hybridoma) cells is greatly enhanced in OVA-treated BMDCs transfected with Hsp25-siRNA and recovered from female C57BL/6 ($H2^b$) mice but not BALB/c ($H2^d$) mice (Fig. 5E). The role of the proteasome was further shown in experiments in which pretreatment with proteasome inhibitor, MG-132, dramatically inhibited IFN-γ release (Fig. 5E). We further showed that Hsp25-plasmid bearing 4T1 tumors grow approximately 3 times larger than Ctrl-plasmid bearing 4T1 tumors or 4T1-wt tumors or 4T1-controlshRNA tumors (Fig. 5F). Taken together, our data suggest that Hsp25/Hsp27 decreases ubiquitination and proteasomal degradation. This is in agreement with

Figure 5. Silencing *hsp25/hsp27* gene expression augments $CD8^+$ T-lymphocyte–dependent tumor killing, recognition and memory responses. A, female BALB/c mice (6–8 weeks old) were injected intraperitoneally with PBS (black lines) or anti-CD4 (L3T4; blue lines), anti-CD8 (Ly-2; red lines), and anti-NK (5E6; green lines) 4 days before injection of 10^4 4T1-controlshRNA cells (left) or 10^4 4T1-Hsp25shRNA cells (right) into the abdominal mammary pads of mice every week. Data represent mean tumor volume ($mm^3 \pm$ SD) and are representative of 4 independently carried out experiments ($n = 3$). B, splenocytes from female BALB/c mice were recovered and $CD8^+$ T cells isolated using negative selection technique according to the manufacturer's instructions (Miltenyi Biotech). Cells (10^6) were stained with 0.5 μg of anti-CD8a (Ly-2), washed and incubated with 0.6 μg of the $F(ab)_2$ anti-rat IgG-FITC (Caltag), and analyzed by flow cytometry. Samples were acquired in a FACScalibur cytometer and analyzed using the Cell Quest Software (Becton Dickinson). A total of 20,000 cells per condition were recorded, and viable cells were defined according to the forward scatter (FSC) and side scatter (SSC) pattern. Data are histograms for the relative number of cells expressing CD8a (Ly-2) and are a representative experiment from 3 independently carried out experiments with similar results. C, 4T1-Hsp25shRNA cells (10^4) were injected into mammary pads of 6- to 8-week-old female BALB/c mice. When tumors started regressing (at the end of 2 weeks), spleens were harvested and $CD8^-$ T cells (open bars) or $CD8^+$ T cells (filled bars) were isolated using negative selection technique according to the manufacturer's instructions (Miltenyi Biotech) and admixed with 4T1-controlshRNA-eGFP(+) cells or 4T1-controlshRNA-eGFP(−) cells or BNL cells which were seeded at various effector:target ratios (10:1, 20:1, and 40:1), in quintuplicate in 96-well tissue culture plates. Cytotoxicity was measured by lactate dehydrogenase-cytotoxicity assay kit II, according to the manufacturer's instructions (BioVision). Bars are the mean percentage of specific lysis (±SD) and are the sum of 4 independently carried out experiments. *, $P < 0.001$ vs. $CD8^-$ cells (Student *t* test). D, 4T1-controlshRNA cells (10^4)-tagged with GFP were injected into the mammary glands of female BALB/c mice on day 0. On day 5, mice were adoptively transferred with $CD8^-$ T cells (rows 1–3 from the top) or $CD8^+$ T cells (rows 4–6 from the top) derived from the spleen of tumor-free female BALB/c mice previously injected with 10^4 4T1-Hsp25shRNA cells. Tumor growth/regression was measured using Maestro *In Vivo* Imaging System. Bars represent the mean GFP signal/exposure (total signal scaled counts/seconds ± SD) from animals adoptively transferred with $CD8^-$ T cells (open bars) or $CD8^+$ T cells (filled bars) and are the sum of 3 mice per group ($n = 3$). *, $P < 0.001$ vs. 4T1-controlshRNA cells (Student *t* test; bottom). E, BMDCs were recovered from female C57BL/6 ($H2^b$) mice (left) or female BALB/c ($H2^d$) mice (right) and transfected with either control-siRNA (open bars) or Hsp25-siRNA (filled bars) or Ctrl-plasmid (hatched bars) or Hsp25-plasmid (gray bars) for 72 hours at 37°C. Cells were then pulsed with 100 ng/mL control peptide (PB1) or 100 ng/mL OVA peptide (S8L) or 10 μmol/L MG-132 for a further 24 hours. Cells were then fixed with paraformaldehyde and admixed with B3Z cells. Bars represent the mean IFN-γ concentration (pg/mL ± SD) and are the sum of 4 independently carried out experiments. *, $P < 0.001$ vs. control-siRNA (Student *t* test). F, on day 0, female BALB/c mice were injected with either 10^5 BNL cells (open squares) or 10^4 4T1-wt cells (open diamonds) or 10^4 4T1-Ctrl-plasmid containing cells (open triangles) or 10^4 4T1-controlshRNA cells (open circles) or 10^4 4T1-Hsp25shRNA cells (filled circles) or 10^4 4T1-Hsp25-plasmid containing cells that stably overexpress Hsp25 using lentivirus gene transfer vector (filled triangles). Tumor growth/regression was measured using an electronic caliper. Sixty days post-TCI, mice previously injected with 4T1-Hsp25shRNA cells were rechallenged with either 10^4 4T1-wt cells (4T1-Hsp25shRNA + 4T1-wt; filled circles) or 10^5 BNL cells (4T1-Hsp25shRNA + BNL; filled squares), and tumor growth was monitored using an electronic caliper. Data are mean tumor volume ($mm^3 \pm$ SD) and are the sum of 2 independently carried out experiment ($n = 5$). FITC, fluorescein isothiocyanate.

Published OnlineFirst December 20, 2011; DOI:10.1158/1940-6207.CAPR-11-0121

recent findings by other scientists (23–27). However, there are other authors who have previously shown that Hsp27 enhances ubiquitination and proteasomal degradation (28–31). The reason for this discrepancy is currently unknown. However, studies using antibodies to pull-down various components of the proteasome complex followed by mass spectrometry and bioinformatics analysis in response to high and low Hsp27 expression are currently underway in our laboratory (Nagaraja et al., manuscript in preparation) and should shed more light on this controversy.

Our additional working hypothesis that high Hsp25 expression represses proteasome activity in turn downregulates peptide loading onto MHC class I molecules for effective recognition by $CD8^+$ T cells is substantiated by data presented in this study. The first suggestion for a role of $CD8^+$ T cells was obtained in experiments in which BALB/c nude mice (which have defective $CD8^+$ and $CD4^+$ T cells) were injected with 4T1-controlshRNA cells that grew approximately 3 times larger than similar cells injected into BALB/c wild-type mice (Fig. 4B). The role of $CD8^+$ T cells was further substantiated in experiments in which the *in vivo* depletion of $CD8^+$ T cells using anti-CD8 (Ly-2) resulted in larger tumors in mice injected with 4T1-controlshRNA and 4T1-Hsp25shRNA cells than in animals injected with isotype control (Fig. 5A). Interestingly, although tumors grew significantly larger in the breast pad of 4T1-Hsp25shRNA–bearing mice in the absence of $CD8^+$ T cells, there were no lung metastases in these mice, as compared with 4T1-controlshRNA–bearing mice (data not shown). Although the possibility exists that the reason for the lack of pulmonary metastasis in 4T1-Hsp25shRNA–bearing mice in the absence of $CD8^+$ T cells is only due to a decrease in primary tumor growth due to enhanced cell death (Supplementary Fig. S1A) and a decrease in proteins associated with cell death (Supplementary Fig. S1D), our *in vitro* data showing that silencing Hsp25 also inhibits migration (Supplementary Fig. S1B), invasion (Supplementary Fig. S1C), and downregulated proteins involved in cell movement (Supplementary Fig. S1D), as well as published data showing that Hsp25 is critical for maintaining the integrity of cytoskeleton (32), suggest that in the absence of specific $CD8^+$ CTL–mediated killing, the tumor is still incapable of leaving the primary tumor foci. Data showing that depletion of NK cells *in vivo* resulted in enhanced antitumor killing and complete tumor regression were initially confounding (Fig. 5A, green lines). However, further examination of the monoclonal antibody used to deplete NK cells *in vivo* revealed it to be the 5E6 Mab $F(ab')_2$ fragment, which reacts with Ly49C, an NK-inhibitory receptor expressed on subsets of NK cells and $NK1.1^+$ or $DX5^+$ T cells in BALB/c mice (33). Studies by Koh and colleagues showed that NK cell–mediated antitumor effector functions are increased against syngeneic tumors *in vitro* and *in vivo* by blockade of the Ly49C and Ly49I inhibitory receptors using the 5E6 monoclonal antibody (34). In addition, the ability of adoptively transferred 4T1-Hsp25shRNA–reactive $CD8^+$ cells, but not $CD8^-$ T cells (non-$CD8^+$ T cells), to rescue mice injected with 4T1-controlshRNA tumors (Fig. 5D), which has been shown to succumb from the tumor burden (Figs. 4A and 4B and 5A), suggest that silencing Hsp25 improved the quality and/or quantity of peptides recognized by $CD8^+$ T cells via a mechanism dependent on enhanced proteasome activity. Conclusive proof that silencing Hsp25 improves the quantity and/or quality of peptides presented onto MHC class I for specific $CD8^+$ T-lymphocyte recognition was obtained indirectly using the *in vitro* cross-presentation assay. Here, we showed that silencing Hsp25 enhances recognition of B3Z (an S8L peptide–specific T-cell hybridoma) cells for OVA-treated BMDCs which have been transfected with Hsp25-siRNA and recovered from female C57BL/6 ($H2^b$) mice but not BALB/c ($H2^d$) mice (Fig. 5E).

The central role of the proteasome is shown in experiments in which IFN-γ release in these cells was drastically blunted by pretreatment with proteasome inhibitor, MG-132 (Fig. 5E). The possibility that silencing Hsp25/27 improves antigen presentation is further substantiated by data showing that Hsp25-siRNA or Hsp27-siRNA treatment of breast cancer cells significantly increased genes important in antigen presentation (Supplementary Fig. S1D). Our studies further showed that silencing Hsp25/27 generates T-cell memory responses. We showed that immunocompetent female BALB/c mice rendered tumor-free by injection with 4T1-Hsp25shRNA can be rechallenged with 4T1-wt or 4T1controlshRNA or 4T1-Ctrl-plasmid–containing cells 60 days after initial challenge without tumor growth (Fig. 5F). However, rechallenge with an irrelevant tumor, BNL cells (a murine-transformed HCC cell line), resulted in tumor growth. The potent efficacious antitumor activities observed by silencing Hsp25 strongly suggest that other antitumor mechanisms have also been activated. This is supported by reports showing that the human homologue of the mouse Hsp25, Hsp27 plays an essential role in (i) stabilizing actin filaments, a structural protein important for maintaining the integrity of cytoskeleton (32), (ii) cell-cycle progression and proliferation (35), and (iii) apoptosis via caspase-3 activation (36, 37). Data from the manuscript suggest that enhanced tumor recognition by $CD8^+$ CTLs may be one of the mechanisms associated with downregulation of Hsp25/27 but does not rule out other pathways. In fact, several studies raise the possibility that the down regulation of Hsp25/27 might activate $CD8^+$ CTL-independent mechanisms associated with HSPs, including findings that the surface expression of Hsp70 in metastatic melanoma (38), acute myeloid leukemia (39), and head and neck cancer (40) stimulates specific NK cell-mediated cytolytic functions are some recent examples. In addition, the development of a Hsp70 peptide which stimulates NK cell-mediated killing of leukemic blast cells (41, 42), and the demonstration that NK cell-mediated targeting of membrane Hsp70 on tumors can be greatly enhanced after treatment

Published OnlineFirst December 20, 2011; DOI:10.1158/1940-6207.CAPR-11-0121

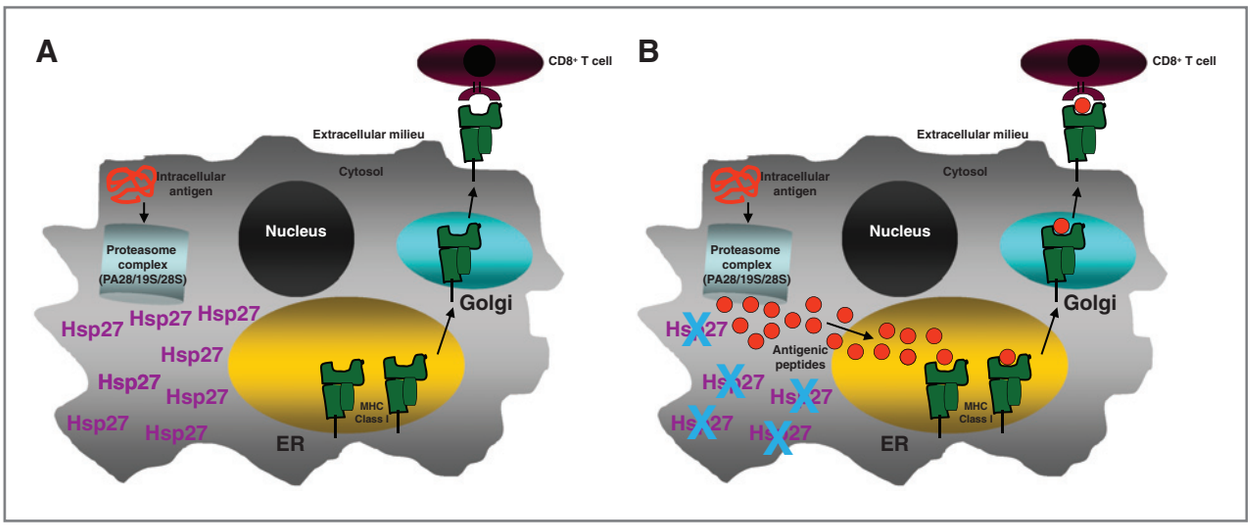

Figure 6. Schematic representation of a hypothetical model by which elevated Hsp25/27 expression in tumors enhances repressed proteasome function, suppresses antigen presentation, and inhibits tumor cell recognition by $CD8^+$ CTLs. In all cells, intracellular antigens or damaged proteins (red coiled lines) found in the cytosol enter the proteasome complex, which contains a PA28, 19S, and 20S subunit (light blue cylinder). A, in breast cancer cells, high levels of Hsp27 inhibit normal proteasome function. This results in inefficient antigenic peptide loading onto MHC class I molecules (green blocks) found in the endoplasmic reticulum (ER) and inability of $CD8^+$ CTL (maroon sphere) to recognize tumors. B, silencing Hsp27 allows antigenic peptides (red circles) to be efficiently transported into the ER, where they bind to MHC class I molecule and are subsequently presented on the cell surface for antigen presentation via the Golgi apparatus. Once at the cell surface, the antigenic peptide–MHC class I complex is scrutinized by $CD8^+$ CTL (maroon sphere). Effective recognition of antigenic peptides by $CD8^+$ CTL activates antitumor immune responses and results in efficient tumor killing and long-lasting memory.

with the cmHsp70.1 monoclonal antibody (43, 44), support the possibility that the down regulation of Hsp25/27 might activate these $CD8^+$ CTL-independent mechanisms.

Taken together, these studies show that increasing proteasome activity of 4T1 breast adenocarcinoma cells by lentivirus-mediated *hsp25* gene silencing or by the transient transfection of siRNA directed against Hsp25 in mice or Hsp27 in human breast cancer cell lines increased specific $CD8^+$ T-lymphocyte tumor killing and enhanced memory responses. The hypothetical model of findings is summarized schematically in Fig. 6. Our data have obvious clinical applications in light of recent successful clinical trials with the proteasome inhibitors. These clinical trials do not contradict our findings because bortezomib resistance is observed in tumors with elevated Hsp27 expression (21). This would suggest that screening for patients on the basis of Hsp27 expression and proteasome activity might add benefit. In addition, this would suggest that combining agents that suppress Hsp27 expression might provide a therapeutic advantage for patients with bortezomib resistance. Clinical trials on the application of siRNA for the treatment of various diseases are underway and early results show it to be safe, with no patients experiencing any serious adverse events (45–47). However, there are current limitations to RNA interference technology primarily in terms of possible "off-target" or nonspecific effects. Off-target effects occur when an siRNA is processed by the RNA-induced silencing complex (RISC) and downregulates an unintended target(s) with similar sequence. An in-depth understanding of how siRNA is metabolized and determining whether intermediate metabolites are toxic or harmful needs to be addressed. Efforts to recognize and circumvent off-target effects for enhanced target identification and to improve the therapeutic application of RNA interference therapy in the clinic are now underway (reviewed in ref. 48).

Disclosure of Potential Conflicts of Interest

No potential conflicts of interest were disclosed.

Acknowledgments

The authors thank Dr. Dider Trono (Ecole Polytechnique Fédérale de Lausanne, Lausanne, Switzerland) for providing the lentivirus plasmids, Dr. Jahangir Kabir for helpful discussions, Dr. Hongying Zheng for expert flow cytometric assistance, and the Scott & White Proteomics Core Facility.

Grant Support

This work was supported in part by Scott & White Memorial Hospital and Clinic Research Advancement Awards (to G.M. Nagaraja and P. Kaur); and the U.S. NIH (RO1CA91889), Scott & White Memorial Hospital and Clinic, the Texas A&M Health Science Center College of Medicine, the Central Texas Veterans Health Administration, and an Endowment from the Cain Foundation (to A. Asea).

The costs of publication of this article were defrayed in part by the payment of page charges. This article must therefore be hereby marked *advertisement* in accordance with 18 U.S.C. Section 1734 solely to indicate this fact.

Received March 8, 2011; revised October 14, 2011; accepted November 1, 2011; published OnlineFirst December 20, 2011.

Published OnlineFirst December 20, 2011; DOI:10.1158/1940-6207.CAPR-11-0121

References

1. Oesterreich S, Hickey E, Weber LA, Fuqua SA. Basal regulatory promoter elements of the hsp27 gene in human breast cancer cells. Biochem Biophys Res Commun 1996;222:155–63.
2. Egeblad M, Werb Z. New functions for the matrix metalloproteinases in cancer progression. Nat Rev Cancer 2002;2:161–74.
3. Soldes OS, Kuick RD, Thompson IA II, Hughes SJ, Orringer MB, Iannettoni MD, et al. Differential expression of Hsp27 in normal oesophagus, Barrett's metaplasia and oesophageal adenocarcinomas. Br J Cancer 1999;79:595–603.
4. Budhram-Mahadeo VS, Heads RJ. Heat shock protein-27 (hsp27) in breast cancers: regulation of expression and function. In: Calderwood SK, Sherman MY, Ciocca DR, editors. Heat shock proteins in cancer. Dordrecht, The Netherlands: Springer; 2007. p. 93–130.
5. O'Neill PA, Shaaban AM, West CR, Dodson A, Jarvis C, Moore P, et al. Increased risk of malignant progression in benign proliferating breast lesions defined by expression of heat shock protein 27. Br J Cancer 2004;90:182–8.
6. Rust W, Kingsley K, Petnicki T, Padmanabhan S, Carper SW, Plopper GE. Heat shock protein 27 plays two distinct roles in controlling human breast cancer cell migration on laminin-5. Mol Cell Biol Res Commun 1999;1:196–202.
7. Ciocca DR, Lo Castro G, Alonio LV, Cobo MF, Lotfi H, Teyssie A. Effect of human papillomavirus infection on estrogen receptor and heat shock protein hsp27 phenotype in human cervix and vagina. Int J Gynecol Pathol 1992;11:113–21.
8. Oesterreich S, Weng CN, Qiu M, Hilsenbeck SG, Osborne CK, Fuqua SA. The small heat shock protein hsp27 is correlated with growth and drug resistance in human breast cancer cell lines. Cancer Res 1993;53:4443–8.
9. Yamamoto K, Okamoto A, Isonishi S, Ochiai K, Ohtake Y. Heat shock protein 27 was up-regulated in cisplatin resistant human ovarian tumor cell line and associated with the cisplatin resistance. Cancer Lett 2001;168:173–81.
10. Storm FK, Mahvi DM, Gilchrist KW. Heat shock protein 27 overexpression in breast cancer lymph node metastasis. Ann Surg Oncol 1996;3:570–3.
11. Thor A, Benz C, Moore D II, Goldman E, Edgerton S, Landry J, et al. Stress response protein (srp-27) determination in primary human breast carcinomas: clinical, histologic, and prognostic correlations. J Natl Cancer Inst 1991;83:170–8.
12. Vargas-Roig LM, Gago FE, Tello O, Aznar JC, Ciocca DR. Heat shock protein expression and drug resistance in breast cancer patients treated with induction chemotherapy. Int J Cancer 1998;79:468–75.
13. Sondel PM, Rakhmilevich AL, de Jong JLO, Hank JA. Cellular immunity and cytokines. In: Mendelsohn J, Howley PM, Israel MA, Liotta LA, editors. The molecular basis of cancer. Philadelphia, PA: W.B. Saunders; 2001. p. 535–71.
14. Kloetzel PM. The proteasome and MHC class I antigen processing. Biochim Biophys Acta 2004;1695:225–33.
15. Groettrup M, Soza A, Eggers M, Kuehn L, Dick TP, Schild H, et al. A role for the proteasome regulator PA28alpha in antigen presentation. Nature 1996;381:166–8.
16. Dick TP, Ruppert T, Groettrup M, Kloetzel PM, Kuehn L, Koszinowski UH, et al. Coordinated dual cleavages induced by the proteasome regulator PA28 lead to dominant MHC ligands. Cell 1996;86:253–62.
17. Sun Y, Sijts AJ, Song M, Janek K, Nussbaum AK, Kral S, et al. Expression of the proteasome activator PA28 rescues the presentation of a cytotoxic T lymphocyte epitope on melanoma cells. Cancer Res 2002;62:2875–82.
18. Stohwasser R, Salzmann U, Giesebrecht J, Kloetzel PM, Holzhutter HG. Kinetic evidences for facilitation of peptide channelling by the proteasome activator PA28. Eur J Biochem 2000;267:6221–30.
19. Whitby FG, Masters EI, Kramer L, Knowlton JR, Yao Y, Wang CC, et al. Structural basis for the activation of 20S proteasomes by 11S regulators. Nature 2000;408:115–20.
20. Pamer E, Cresswell P. Mechanisms of MHC class I–restricted antigen processing. Annu Rev Immunol 1998;16:323–58.
21. Chauhan D, Li G, Shringarpure R, Podar K, Ohtake Y, Hideshima T, et al. Blockade of Hsp27 overcomes Bortezomib/proteasome inhibitor PS-341 resistance in lymphoma cells. Cancer Res 2003;63:6174–7.
22. Mitsiades N, Mitsiades CS, Poulaki V, Chauhan D, Fanourakis G, Gu X, et al. Molecular sequelae of proteasome inhibition in human multiple myeloma cells. Proc Natl Acad Sci U S A 2002;99:14374–9.
23. Andrieu C, Taieb D, Baylot V, Ettinger S, Soubeyran P, De-Thonel A, et al. Heat shock protein 27 confers resistance to androgen ablation and chemotherapy in prostate cancer cells through eIF4E. Oncogene 2010;29:1883–96.
24. Trott D, McManus CA, Martin JL, Brennan B, Dunn MJ, Rose ML. Effect of phosphorylated hsp27 on proliferation of human endothelial and smooth muscle cells. Proteomics 2009;9:3383–94.
25. Knapinska AM, Gratacos FM, Krause CD, Hernandez K, Jensen AG, Bradley JJ, et al. Chaperone Hsp27 modulates AUF1 proteolysis and AU-rich element-mediated mRNA degradation. Mol Cell Biol 2011;31:1419–31.
26. Chang E, Heo KS, Woo CH, Lee H, Le NT, Thomas TN, et al. MK2 SUMOylation regulates actin filament remodeling and subsequent migration in endothelial cells by inhibiting MK2 kinase and HSP27 phosphorylation. Blood 2011;117:2527–37.
27. de Thonel A, Vandekerckhove J, Lanneau D, Selvakumar S, Courtois G, Hazoume A, et al. HSP27 controls GATA-1 protein level during erythroid cell differentiation. Blood 2010;116:85–96.
28. Parcellier A, Brunet M, Schmitt E, Col E, Didelot C, Hammann A, et al. HSP27 favors ubiquitination and proteasomal degradation of p27Kip1 and helps S-phase re-entry in stressed cells. FASEB J 2006;20:1179–81.
29. Parcellier A, Schmitt E, Gurbuxani S, Seigneurin-Berny D, Pance A, Chantome A, et al. HSP27 is a ubiquitin-binding protein involved in I-kappaBalpha proteasomal degradation. Mol Cell Biol 2003;23:5790–802.
30. Friant S, Meier KD, Riezman H. Increased ubiquitin-dependent degradation can replace the essential requirement for heat shock protein induction. EMBO J 2003;22:3783–91.
31. den Engelsman J, Keijsers V, de Jong WW, Boelens WC. The small heat-shock protein alpha B-crystallin promotes FBX4-dependent ubiquitination. J Biol Chem 2003;278:4699–704.
32. Guay J, Lambert H, Gingras-Breton G, Lavoie JN, Huot J, Landry J. Regulation of actin filament dynamics by p38 map kinase-mediated phosphorylation of heat shock protein 27. J Cell Sci 1997;110:357–68.
33. Yu YY, George T, Dorfman JR, Roland J, Kumar V, Bennett M. The role of Ly49A and 5E6(Ly49C) molecules in hybrid resistance mediated by murine natural killer cells against normal T cell blasts. Immunity 1996;4:67–76.
34. Koh CY, Blazar BR, George T, Welniak LA, Capitini CM, Raziuddin A, et al. Augmentation of antitumor effects by NK cell inhibitory receptor blockade *in vitro* and *in vivo*. Blood 2001;97:3132–7.
35. Farooqui-Kabir SR, Budhram-Mahadeo V, Lewis H, Latchman DS, Marber MS, Heads RJ. Regulation of Hsp27 expression and cell survival by the POU transcription factor Brn3a. Cell Death Differ 2004;11:1242–4.
36. Rocchi P, Beraldi E, Ettinger S, Fazli L, Vessella RL, Nelson C, et al. Increased Hsp27 after androgen ablation facilitates androgen-independent progression in prostate cancer via signal transducers and activators of transcription 3-mediated suppression of apoptosis. Cancer Res 2005;65:11083–93.
37. Rocchi P, Jugpal P, So A, Sinneman S, Ettinger S, Fazli L, et al. Small interference RNA targeting heat-shock protein 27 inhibits the growth of prostatic cell lines and induces apoptosis via caspase-3 activation *in vitro*. BJU Int 2006;98:1082–9.
38. Farkas B, Hantschel M, Magyarlaki M, Becker B, Scherer K, Landthaler M, et al. Heat shock protein 70 membrane expression and melanoma-associated marker phenotype in primary and metastatic melanoma. Melanoma Res 2003;13:147–52.
39. Gehrmann M, Schmetzer H, Eissner G, Haferlach T, Hiddemann W, Multhoff G. Membrane-bound heat shock protein 70 (Hsp70) in acute

Published OnlineFirst December 20, 2011; DOI:10.1158/1940-6207.CAPR-11-0121

myeloid leukemia: a tumor specific recognition structure for the cytolytic activity of autologous NK cells. Haematologica 2003;88:474–6.

40. Kleinjung T, Arndt O, Feldmann HJ, Bockmuhl U, Gehrmann M, Zilch T, et al. Heat shock protein 70 (Hsp70) membrane expression on head-and-neck cancer biopsy-a target for natural killer (NK) cells. Int J Radiat Oncol Biol Phys 2003;57:820–6.
41. Gross C, Holler E, Stangl S, Dickinson A, Pockley AG, Asea AA, et al. An Hsp70 peptide initiates NK cell killing of leukemic blasts after stem cell transplantation. Leuk Res 2008;32:527–34.
42. Stangl S, Gross C, Pockley AG, Asea AA, Multhoff G. Influence of Hsp70 and HLA-E on the killing of leukemic blasts by cytokine/Hsp70 peptide-activated human natural killer (NK) cells. Cell Stress Chaperones 2008;13:221–30.
43. Stangl S, Gehrmann M, Dressel R, Alves F, Dullin C, Themelis G, et al. *In vivo* imaging of CT26 mouse tumours by using cmHsp70.1 monoclonal antibody. J Cell Mol Med 2011;15:874–87.
44. Stangl S, Gehrmann M, Riegger J, Kuhs K, Riederer I, Sievert W, et al. Targeting membrane heat-shock protein 70 (Hsp70) on tumors by cmHsp70.1 antibody. Proc Natl Acad Sci U S A 2011;108:733–8.
45. DeVincenzo J, Lambkin-Williams R, Wilkinson T, Cehelsky J, Nochur S, Walsh E, et al. A randomized, double-blind, placebo-controlled study of an RNAi-based therapy directed against respiratory syncytial virus. Proc Natl Acad Sci U S A 2010;107:8800–5.
46. Leachman SA, Hickerson RP, Schwartz ME, Bullough EE, Hutcherson SL, Boucher KM, et al. First-in-human mutation-targeted siRNA phase Ib trial of an inherited skin disorder. Mol Ther 2010;18:442–6.
47. Kaiser PK, Symons RC, Shah SM, Quinlan EJ, Tabandeh H, Do DV, et al. RNAi-based treatment for neovascular age-related macular degeneration by Sirna-027. Am J Ophthalmol 2010;150:33–9.e2.
48. Jackson AL, Linsley PS. Recognizing and avoiding siRNA off-target effects for target identification and therapeutic application. Nat Rev Drug Discov 2010;9:57–67.